

Crystal growth of intermediate-molecular-mass poly(ethylene oxide) fractions from the melt

Stephen Z. D. Cheng, Jianhua Chen and James J. Janimak

Institute and Department of Polymer Science, College of Polymer Science and Polymer Engineering, The University of Akron, Akron, Ohio 44325-3909, USA

(Received 1 March 1989; revised 12 June 1989; accepted 3 July 1989)

Linear crystal growth rates of poly(ethylene oxide) (PEO) fractions crystallized from the melt have been measured in an intermediate-molecular-mass range ($MW = 23\,000\text{--}105\,000$). Regime phenomena have been observed during crystallization. Regime II/III transitions occur at $\Delta T = 17.5 \pm 0.5$ K and regime I/II transitions appear at $\Delta T = 10 \pm 0.5$ K for those fractions for which the equilibrium melting temperature of 342.2 K for PEO crystals is used. Interestingly, we have found that in these PEO fractions reversion from regime I back to regime II exists even at a lower supercooling of 8.5 ± 0.5 K. Detailed kinetic analyses of the data demonstrate the suitability of the present nucleation theory. The molecular-mass dependence of the PEO fraction has also been discussed. Morphological changes can be observed along with regime transitions of PEO crystal growth.

(Keywords: crystal growth; crystallization; hedrite; intermediate molecular mass; kinetics; morphology; nucleation; poly(ethylene oxide) fraction; regime; spherulite; surface free energy; supercooling)

INTRODUCTION

During the last 20 years, poly(ethylene oxide) (PEO) has been one of the most extensively studied crystalline polymers. In particular, the melt-crystallization behaviour of PEO fractions in its low-molecular-mass range is most interesting. Kovacs *et al.* have presented a series of systematic reports on the crystal growth rates and morphology of PEO fractions crystallized from the melt as observed by optical microscopy (OM)¹⁻⁵. The molecular-mass range in their study was between $MW = 2000$ and $10\,000$. It is now well known that the low-molecular-mass PEO fractions crystallized from the melt at low supercooling form lamellar single crystals with chains either fully extended or folded a small integer number of times¹⁻⁵. In both cases the OH-terminated chain ends are therefore rejected onto the surface layers of the lamellae. The number m of folds per molecule depends upon crystallization temperature and time. During isothermal crystallization or annealing, the lamellar thickness of m -folded chain crystals increases in a stepwise manner ($(m-1)$ -folded chain crystals) owing to the quantized reduction of m .

Recently, the study of binary mixtures of PEO fractions was carried out in order to pursue the idea of molecular nucleation⁶⁻⁹. In that study, the low-molecular-mass fractions used were below $MW = 15\,000$ and the high-molecular-mass fractions were above $MW = 100\,000$. Wunderlich *et al.* have found that molecular segregation in those mixtures occurs before the temperature reaches the equilibrium melting point of the low-molecular-mass fraction, indicating a process in which every molecule has to pass through its own nucleation step at least once⁶⁻⁹. A new etching method has been developed in order to observe such molecular segregation via transmission electron microscopy (TEM)^{8,10,11}. A double-

lamellar morphology has also been reported in low-molecular-mass PEO fractions when the crystals have an odd number of folds per molecule¹².

A more detailed study has led to a closer look at the growth kinetics of low-molecular-mass PEO fractions crystallized from the melt. The supercooling (temperature) and molecular-mass dependences are evident. A new description of such kinetics with respect to the molecular-mass dependence is:

$$\log v_c = A \log(\ln n) + B \quad (1)$$

at constant supercooling, where n is the degree of polymerization, and A and B are constants. From equation (1), one term is molecular-mass-dependent and the other is not. More interestingly, a transition between non-integral folding and integral folding can be clearly seen based on molecular mass and supercooling¹³. For 15 PEO fractions, we have found that such a transition occurs at low supercoolings.

In the 1970s, several reports of linear crystal growth rates and overall crystallization rates of PEO fractions in the molecular-mass range of 10^4 to 10^6 appeared, with polydispersities between 1.2 and 2.0^{14,15}. Using reported literature values, Allen and Mandelkern recently reported that there is a transition between regimes I and II in those PEO fractions at $\Delta T = 24$ K, if the equilibrium melting temperature of PEO crystals was taken to be 353.7 K^{16,17}. It is the first time that the existence of regime behaviour in PEO crystal growth has been pointed out. Furthermore, they reported that there is no clear correlation between the regime transition and morphological changes in the PEO fractions¹⁷.

Our intention is to focus on an intermediate-molecular-mass range between 1.5×10^4 and 1.5×10^5 and to study the crystal growth behaviour of PEO fractions with very

narrow molecular-mass distributions (polydispersities ≤ 1.05). In this molecular-mass range, it is known that integral folding chain crystals will not appear and, therefore, normal crystal growth behaviour of the PEO fractions should be predicted. On the other hand, we have understood quite clearly that regime phenomena have been observed in both polyethylene (PE)¹⁸ and polyoxymethylene (POM)¹⁹ cases, in which PE shows three regimes (regimes I, II and III) and POM shows two regimes (regimes II and III). This raises the question: Can we observe similar regime phenomena, in particular, regime III, in PEO, which has a chemical structure between PE and POM?

In this paper, we will report our very recent study of linear crystal growth of PEO fractions from the melt in that intermediate-molecular-mass range. It is now evident that regime phenomena can also be observed in these PEO fractions. The supercooling at the transition between regimes II and III is 17.5 ± 0.5 K, and that of the transition between regimes I and II is 10 ± 0.5 K. Of special interest is the transition from regime I back to regime II at an even lower supercooling of 8.5 ± 0.5 K for the PEO fractions. Possible explanations will be explored. The polarized optical microscopic study also shows that there are morphological changes between regimes II and III (at $\Delta T = 17.5 \pm 0.5$ K) and between regimes I and II (at $\Delta T = 10 \pm 0.5$ K and $\Delta T = 8.5 \pm 0.5$ K).

EXPERIMENTAL

Materials and samples

The PEO fractions were purchased from Polysciences Inc. and Polymer Laboratories Ltd. The molecular characterization data are listed in Table 1. This table also shows the equilibrium melting temperature, T_m° , of these samples, as calculated by the following equation:

$$T_m^\circ(MW) = T_m^\circ [n \Delta h_f - \sigma_e(1 + \alpha T_0)] / (n \Delta h_f + RT_m^\circ \ln n - \alpha \sigma_e T_m^\circ) \quad (2)$$

where the heat of fusion of the monomer units $\Delta h_f = 8.67$ kJ mol⁻¹, $T_m^\circ = 342.2$ K and $\alpha = 1.29 \times 10^{-2}$ K⁻¹. For the surface free energy of extended-chain crystals, in the vicinity of the reference temperature, $T_0 = 334.4$ K, $\sigma_e = 6.57$ kJ mol⁻¹.

All of the samples were carefully dried under vacuum prior to investigation. About 5–10 mg of the PEO was melted on a hot plate, and inserted between two, 0.15 mm thick, coverslips (60×12 mm²). The thickness of the polymer film (~ 10 μ m) was controlled by an aluminium film (with a thickness of 10 μ m) which was put in between the slips. The sandwiched specimens were then stored under vacuum at room temperature before their final heat treatment and measurement.

Table 1 Molecular characterization for poly(ethylene oxide) fractions

Fractions	\bar{M}_n	\bar{M}_w/\bar{M}_n	T_m° ^a (K)	Chain length ^b (nm)
2.30×10^4	2.30×10^4	1.04	340.4	145.4
5.63×10^4	5.63×10^4	1.05	341.4	335.9
1.05×10^5	1.05×10^5	1.05	341.7	663.7

^a Calculated based on equation (2) in text

^b Chain length = M_n/d ; $d = 158.2$ g nm⁻¹ (ref. 3)

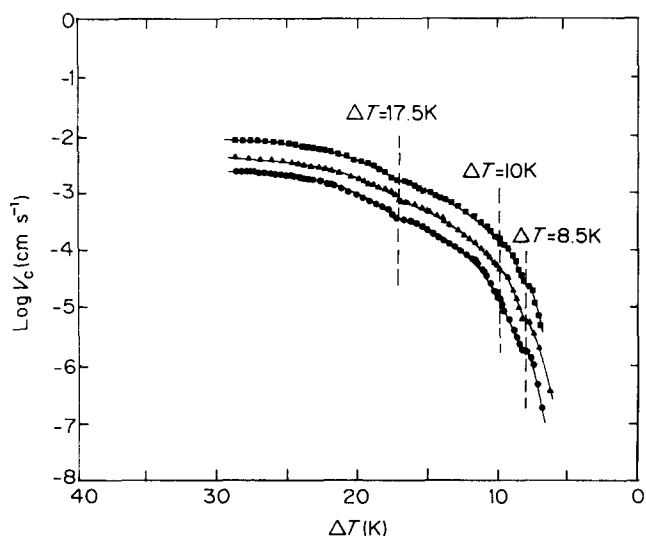


Figure 1 The relationship between the logarithmic linear crystal growth rate ($\log v_c$) of three poly(ethylene oxide) fractions crystallized from the melt and the supercooling (ΔT). $MW = \blacksquare$, 23 000, \blacktriangle , 56 300; \bullet , 105 000. The vertical broken lines are the cross-over points between two growth rate curves (see text)

Polarized optical microscopy

A polarized optical microscope (OM) (Nikon Labo-phot-pol) was used in conjunction with a Mettler hot stage (FP-52). The specimens were heated to 373.2 K on the hot plate for 2 min, and were then inserted into the hot stage at a pre-fixed temperature as quickly as possible. After the hot stage reached thermal equilibrium, the crystal growth rates were measured.

In the low supercooling range, a self-seeding technology was used by following the method of Kovacs *et al.*¹. The simplest procedure is that the specimens were (i) molten at 373.2 K, (ii) cooled to 318.2 K where crystallization occurs rapidly and then (iii) reheated (0.2 K min⁻¹) in a reproducible manner to a temperature T_s , which is slightly lower than T_m° (typically, $T_m^\circ - T_s \approx 1-2$ K), where the major part of the PEO materials melt—often slowly—except the seeds, which represent a volume fraction of the order of 0.001% or less. After a pre-determined length of time for the specimens at T_s , the specimens were inserted into the hot stage at a pre-fixed temperature for the measurement of crystal growth rates. Each data point of the growth rates was the average of five repeated measurements.

In order to study the change of morphology in the PEO fractions with supercooling, photographs were taken with a 35 mm camera.

Finally, the hot stage was calibrated with standard, sharp-melting substances. Its temperature control was better than ± 0.1 K. The crystallization was recorded by a timer.

RESULTS AND DISCUSSION

Crystal growth rate and regime analyses

Figure 1 represents the relationship between the logarithmic linear crystal growth rate and supercooling (ΔT) for the PEO fractions. It is clear that for the PEO fractions there are four individual growth-rate curves separated by three cross-over points. These intersecting points correspond to supercoolings of 8.5, 10 and 17.5 K,

respectively, indicated by the vertical broken lines in the figure. This is surprising since even the three crystal growth regimes based on Hoffman's suggestion^{18,20} need only two cross-over points.

Disregarding this apparent contradiction, let us first follow regime analyses^{18,20} to treat our experimental data shown in Figure 1, as one alternative. Generally speaking, the growth rate of polymers during crystallization is described in a given regime by the equation^{18,20}:

$$v_c = v_0(\Delta T) \exp[-U^*/R(T_c - T_\infty)] \exp[-K_g/T_c(\Delta T)f] \quad (3)$$

Taking the logarithm of equation (3), one obtains:

$$\log v_c = \log v_0 + \log(\Delta T) - U^*/2.303R(T_c - T_\infty) - K_g/2.303T_c(\Delta T)f \quad (4)$$

where $f = 2T_c(T_m^\circ + T_c)$, $K_g(\text{regimes I, III}) = 4b\sigma_e T_m^\circ/k \Delta h_f$ and $K_g(\text{regime II}) = 2b\sigma_e T_m^\circ/k \Delta h_f$, T_c is the crystallization temperature, T_m° is the equilibrium melting temperature for a particular molecular mass (see Table 1), σ is the lateral surface free energy, σ_e is the fold surface free energy, b is the lattice parameter in the growth direction ($b = 0.462$ nm for the lattice distance between adjacent (120) planes) and k if the Boltzmann constant. The pre-exponential term v_0 has recently been defined as $Z/n^{1+\lambda}$, which introduces the mobility, diffusion or jump-rate effect, and n is the degree of polymerization (it has been claimed that using n_z here yields a better fit compared to using n_w)²⁰. The value of λ is defined as $\pi/2\phi$ where ϕ is the angle of sweep in radians of the first chain after it has achieved its first attachment. The quantity U^* is the activation energy of reptation in the melt. In the case of PEO, we tried two values: 29.3 kJ mol^{-1} , quoted by Kovacs *et al.*¹⁻⁵, and 6.28 kJ mol^{-1} , the empirical 'universal' value suggested by Hoffman²¹. Finally, the value of T_∞ was chosen by the definition of $T_g - 30 \text{ K}$ with the T_g of PEO at 206 K . A plot of $\log v_0 + U^*/2.303R(T_c - T_\infty) - \log(\Delta T)$ vs. $1/T_c(\Delta T)f$ can thus provide the value of K_g (slope) and v_0 (intersection) for each regime.

Figure 2 represents the plots for these PEO fractions by applying Kovacs' value ($U^* = 29.3 \text{ kJ mol}^{-1}$). It is interesting to note that, instead of the regularly described normal three growth regimes, four regimes can be seen. The transition between regimes II and III for the PEO fractions is at $17.5 \pm 0.5 \text{ K}$, that between regimes I and II at $10 \pm 0.5 \text{ K}$. At a low supercooling of $8.5 \pm 0.5 \text{ K}$, there is apparently another reversion from regime I back to regime II. This high-temperature regime is judged by curve fitting to have a slope close to but slightly larger than the slope of regime II between $\Delta T = 10$ and 17.5 K , indicating that this regime is basically a regime II growth, but mixed with a little regime I growth. On the other hand, such a reversion also affects the growth behaviour in regime I. It is evident that the slopes in regime I are 10–16% smaller than those in regime III, indicating that the crystal growth behaviour of the PEO fractions between $\Delta T = 10$ and 8.5 K mainly belongs to regime I, but is also mixed with some of regime II growth. Assuming that the summation of the two slope ratios is close to 4, as Phillips *et al.* predicted²², one may expect that the values of $K_g(\text{I})$ for the PEO fractions should be -0.222×10^5 , -0.251×10^5 and -0.254×10^5 , respectively. Therefore, we can forecast the percentages of regime II growth that remain in the supercooling range between

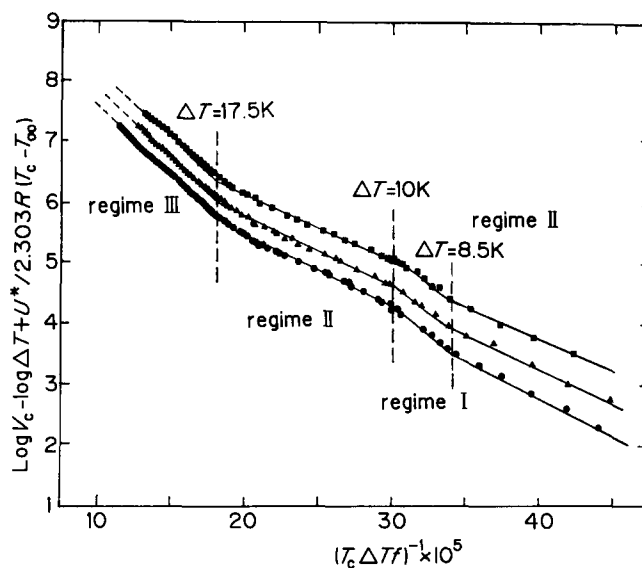


Figure 2 Plot of $\log v_c + U^*/2.303R(T_c - T_\infty) - \log \Delta T$ vs. $1/T_c(\Delta T)f$ for three poly(ethylene oxide) fractions crystallized from the melt. $MW = \blacksquare$, 23 000; \blacktriangle , 56 300; \bullet , 105 000. Regime phenomena can be observed. In particular, a reversion from regime I back to regime II at $\Delta T = 8.5 \pm 0.5 \text{ K}$ for the PEO fractions can be clearly seen. For the plots, $U^* = 29.3 \text{ kJ mol}^{-1}$, $T_\infty = T_g - 30 \text{ K}$ and T_m° is calculated from equation (2) in the text. The linear crystal growth rate v_c is in cm s^{-1} .

10 and 8.5 K , namely 35%, 43% and 39% for those three fractions, respectively, if these two growth regimes are treated as being independent. Similar predictions can be applied to the reversion from regime I back to regime II. The percentages of regime I growth are 4%, 5% and 5%, respectively, for the three PEO fractions below $\Delta T = 8.5 \text{ K}$.

Detailed data of the slopes, the products of lateral and fold surface free energies, $\sigma\sigma_e$, the ratios between two neighbouring regimes and other parameters for the PEO fractions are listed in Table 2. The values of $\sigma\sigma_e$ in both low supercooling regimes, designated as I(II) and II(I) in Table 2, are calculated based on an addition scheme of the percentages of two different growth regimes as described previously. To apply the empirical 'universal' value ($U^* = 6.28 \text{ kJ mol}^{-1}$) obscures those regime transitions, in particular, at the low-molecular-mass size ($MW = 23 000$). A similar observation has been reported by Phillips *et al.* in the case of *cis*-polyisoprene (*cis*-PI)²².

Of particular interest is the regime II/III transition of the PEO fractions at $\Delta T = 17.5 \pm 0.5 \text{ K}$. Such a transition phenomenon was first observed and plotted by Kovacs *et al.* in 1977 (figure 15 in ref. 3). For the high-molecular-mass PEO ($MW = 150 000$) there is a clear upper deviation of the slope at about $\Delta T = 17 \text{ K}$, which they did not discuss in their report. Such a deviation leads to a new slope in the lower supercooling range, and the ratio between these two slopes is in the vicinity of 2. The explanation given now shows that there is evidence for the existence of regime III in the high supercooling range.

For the surface free energies, if one assumes that $\sigma \approx 10 \text{ erg cm}^{-2}$, the fold surface free energy σ_e is thus in the range of $26\text{--}30 \text{ erg cm}^{-2}$ based on the data in Table 2, and it is in good agreement with Kovacs' estimation from melting data, from which in the vicinity of 333.2 K the fold surface free energy is 22.4 erg cm^{-2} . For the data given by Kovacs in ref. 3, one can find that their $\sigma\sigma_e$ should be $225 \text{ erg}^2 \text{ cm}^{-4}$ instead of $450 \text{ erg}^2 \text{ cm}^{-4}$ if we use the regime III approach, and therefore their data again fit

Table 2 Kinetic data of poly(ethylene oxide) fractions crystallized from the melt

MW	Regimes ^a	$K_g \times 10^5$ (K ⁻²)	$\sigma\sigma_e$ (erg ² cm ⁻⁴)	q^b (kJ mol ⁻¹)	Ratio ^c
2.3×10^4	II(I)	-0.114 ± 0.02	266	6.8	1.605
	I(II)	-0.183 ± 0.02	269	6.9	1.664
	II	-0.110 ± 0.02	267	6.9	1.982
	III	-0.218 ± 0.02	264	6.8	
5.63×10^4	II(I)	-0.125 ± 0.02	288	7.4	1.552
	I(II)	-0.194 ± 0.02	299	7.7	1.630
	II	-0.119 ± 0.02	288	7.4	1.899
	III	-0.226 ± 0.02	273	7.0	
1.05×10^5	II(I)	-0.130 ± 0.02	299	7.7	1.554
	I(II)	-0.202 ± 0.02	303	7.8	1.683
	II	-0.120 ± 0.02	290	7.5	1.892
	III	-0.227 ± 0.02	274	7.1	

^a The designation II(I) (or I(II)) means that in that regime the main growth behaviour is in regime II (or I), but mixed with some regime I (or II) growth; see text

^b The calculation assumes $\sigma = 10 \text{ erg cm}^{-2}$

^c The values of ratios between two slopes are based on $K_g(\text{III})/K_g(\text{II})$, $K_g(\text{I(II)})/K_g(\text{II})$ and $K_g(\text{II(I)})/K_g(\text{II(I)})$

very well to our data listed in *Table 2*. It is also interesting to note that the fold surface free energy σ_e decreases slightly with molecular mass in all the regimes, indicating a gradual change of chain-folding regularity with respect to the molecular mass of the PEO fractions. The work of chain folding is obtained directly from the fold surface free energy as²¹:

$$q = 2\sigma_e A \quad (5)$$

where A is the molecular cross-sectional area, and for PEO this is 0.214 nm^2 . The values of q for different molecular-mass fractions are also listed in *Table 2*. It is worth noting that all the values of q listed are quite comparable to (even smaller than) typical values of q for flexible chains ($\sim 12.6 \text{ kJ mol}^{-1}$), revealing the flexible nature of the PEO chain molecules.

The question that still remains is why at low supercoolings one can observe such a reversion from regime I back to regime II. A similar observation was reported by Phillips *et al.* in the case of *cis*-PI²². However, compared to Phillips' interpretation for the reappearance of regime II, we believe that, since our PEO samples have very narrow polydispersities, molecular segregation may not have a major influence on crystal growth in regime I. Other alternatives were proposed to Goldenfeld²³ and Hoffman²⁴. The key point in their explanations is that the substrate length L during polymer crystal growth in regime I should be so extensive that multiple nucleation inevitably results, producing a reversion to regime II growth, although in their approaches the causes of such an extension of L are different. Goldenfeld pointed out that the possibility of changing the nucleation rate i and the substrate completion rate g may lead to an inherently unstable growth in regime I²³. Hoffman proposed, on the other hand, that such a reversion should be observed at lower supercooling as soon as the lifetime of an 'Ω defect' is shorter than the residence time of the substrate²⁴. More recently, Hoffman and Miller²⁰ have suggested that the substrate length L must be connected with the stem correlation length of the polymer crystals measured from the X-ray linewidth. The precise physical origin of this stem correlation length is not known, although one could suppose that it might well have certain relevance to strain resulting from repulsion of chain folds. Therefore, one may regard the possibility that L and the X-ray stem correlation length have

a natural relationship. Defects (semi-one-dimensional defects) can thus be introduced to stop crystal completion at low supercooling. Nevertheless, the defects may also be annealed away from crystal surfaces before crystal completion at even lower supercooling; the substrate length L increases, thus explaining such reversion from regime I back to regime II.

An alternative approach to nucleation theory was proposed by the late Dr D. M. Sadler²⁵. He proposed that the regime transitions can be better understood by his rough surface growth (RSG) model. Those transitions may be attributed to the so-called 'pinning' points or 'poisoning' phenomena introduced by conformational impurities during crystal growth. Before making any comment on the RSG model, we must state that it has to be quantitatively tested in a broader base of experimental observations.

Our observations on the reversion from regime I back to regime II reveals systematically for the first time that such reversion occurs at the same supercooling (8.5 K) in this molecular-mass range. In this regime, one can find that the slopes for the PEO fractions are very close to those in regime II, as listed in *Table 2*, but different values of the pre-exponential factor, $\log v_0$, have been found. In order to develop a full explanation of such reversion, one needs a further in-depth study into PEO morphology and growth habits, which is currently being undertaken by our research group.

Finally, if one now changes the equilibrium melting temperatures to 353.7 K ^{16,17} and fixes all the other kinetic parameters, the regime phenomena in those PEO fractions can still be observed, but the slopes (K_g) and the intersections ($\log v_0$) are changed. As a result, the products of surface free energies increase to about $660 \text{ erg}^2 \text{ cm}^{-4}$. Again, assuming $\sigma \approx 10 \text{ erg cm}^{-2}$ as before, this leads to a fold surface free energy σ_e of $\sim 66 \text{ erg cm}^{-2}$, which is about 2.5 times higher than Kovacs' estimation and 1.5 times higher than Hoffman's estimation ($\bar{\sigma}_e \approx 42.2 \text{ erg cm}^{-2}$ for PEO crystals of double lamellae)²⁶, but still in the same order of magnitude.

Crystal growth rates as a function of molecular mass

As reviewed in ref. 7, several attempts have been made to discuss the molecular-mass dependence of crystal

growth rate in polymers crystallized from the melt²⁷⁻³⁰. Very recently, it has been proposed by Hoffman and Miller²⁰, based on the reptation concept³¹, that at a constant supercooling the crystal growth rates of PE as a function of molecular mass can be described by:

$$\log v_c = C \log n_z + D \quad (6)$$

where $C = -4/3$ in regime I and $C = -7/6$ in regime II. All other terms are included in the constant D . Here n_z is the Z-average degree of polymerization. Comparing equation (6) with equation (1), one can see their similarities. In fact, as we have indicated elsewhere¹³, when one considers cooperative models, power laws (n^γ) are most often observed rather than logarithmic expressions ($\ln n$)⁴ as in equation (1). Assuming that n^γ expresses the molecular-mass dependence of a cooperative process, one can, via $n^\gamma = (e^{\ln n})^\gamma = e^{\gamma \ln n}$, write n^γ approximately as $1 + \gamma \ln n$ if γ is small. After the expansion of n^γ , equation (1) would then take the form:

$$\log v_c = K\gamma \ln n + B \quad (7)$$

Equation (7) thus has the same format of equation (6) even though both equations have their own theoretical background.

Figure 3 shows plots of $\log v_c$ vs. $\log n$ for the PEO fractions at different supercoolings. One can find well defined linear relationships between these two quantities. From equation (6), one should predict a constant slope within one regime. The slope changes only when the regime changes. From our observations, however, the slope change also occurs within one regime as shown in Figure 3. In particular, at the low supercooling above the reversion of regime I back to regime II, namely at $\Delta T = 7.7$ K, the slope is indeed close to the slopes in regime II (ΔT between 10 and 17.5 K), rather than the slope found in regime I. Furthermore, the slopes of the plots in regime II are even smaller. This should indicate that, in regime III, only segmental diffusion becomes possible. In addition to reptational motion, a cooperative model might be helpful.

Morphological changes at the supercooling of regime transitions

As described above, crystal growth of the PEO fractions in the intermediate-molecular-mass range ex-

hibits regime phenomena. At $\Delta T = 17.5 \pm 0.5$ K, regime II/III transitions can be observed; at $\Delta T = 10 \pm 0.5$ K, regime I/II transitions occur; finally, at $\Delta T = 8.5 \pm 0.5$ K, a reversion transition of regime I back to regime II can be found. We have focused on the vicinity of these three supercoolings and the morphological changes of the PEO fractions. Figure 4 shows the crystalline morphology at five different supercoolings ($\Delta T = 18.5, 16.5, 11, 9.5$ and 7.5 K, respectively) for one PEO fraction ($MW = 105\,000$), as an example. It is evident that, through the transitions between regimes II and III at $\Delta T = 17.5 \pm 0.5$ K, the morphological change is mainly documented by the disappearance of the Maltese cross pattern as shown in the change from Figure 4a to 4b. Note that such a change is only within 2 K. In regime III, therefore, the crystalline morphology is spherulitic, and in the upper limit of regime II we address such morphology as an intermediate state. One must, however, also study Figure 4c to see whether the intermediate state is dominant in the whole regime II, since Figure 4c lies at the lower limit of supercooling (11 K) in this regime. In comparison the morphological change in this supercooling range (7.5 K) is quite gradual and obscure, but still in this intermediate state. Nevertheless, one can observe a change in birefringence, and the crystal texture becomes increasingly coarse. During the transition between regimes II and I, the morphological change is represented in Figures 4c and 4d. Within $\Delta T = 1.5$ K, one can find that a finer texture is prominent in regime I, which closely resembles a hedrite texture. Finally, through the reversion from regime I to regime II, Figure 4e shows a texture that is close to a single crystal of a PEO fraction. Indeed, for the PEO fraction of $MW = 23\,000$, we have occasionally observed single-crystal-like textures below $\Delta T = 8.5$ K. Overall, such observations indicate that, during regime transitions of PEO crystal growth in this molecular-mass range, morphological changes can be observed in OM. In order to ascertain whether those regime transitions accompany texture changes in a finer size scale, say, for example, in the order of nanometres, one needs to study further the texture observations via transmission electron microscopy, which is currently being undertaken in our research laboratory with our new etching method^{8,10,11}.

CONCLUSIONS

We have reported in this work a detailed study of crystal growth habits of three PEO fractions in an intermediate-molecular-mass range. The polydispersities of the fractions are very narrow, and therefore molecular segregation should not be a major factor in this study, particularly in the low supercooling region. The conclusions we have reached are as follows.

When we apply the nucleation theory, the PEO fractions studied here exhibit regime phenomena during crystallization from the melt. All three regimes have been observed, at $\Delta T = 17.5 \pm 0.5$ K for regime II/III transitions and $\Delta T = 10 \pm 0.5$ K for regime I/II transitions.

A reversion from regime I back to regime II has been identified at $\Delta T = 8.5 \pm 0.5$ K for the PEO fractions. Such a reversion disturbs regime I growth between $\Delta T = 10$ and 8.5 K and leads to a mixture of both regime I and regime II growths. On the other hand, below $\Delta T = 8.5$ K, we can also find that the growth behaviour contains a slight regime I growth (up to 5%).

The molecular-mass dependence of PEO crystal growth

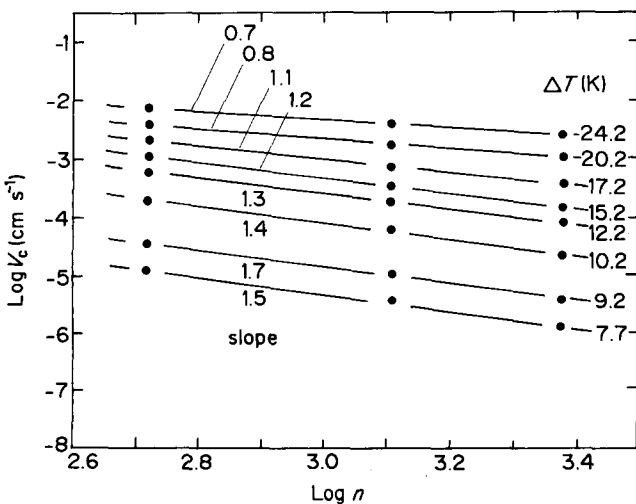


Figure 3 The relationship between the logarithmic crystal growth rate ($\log v_c$) and the logarithmic degree of polymerization ($\log n$) at different supercoolings

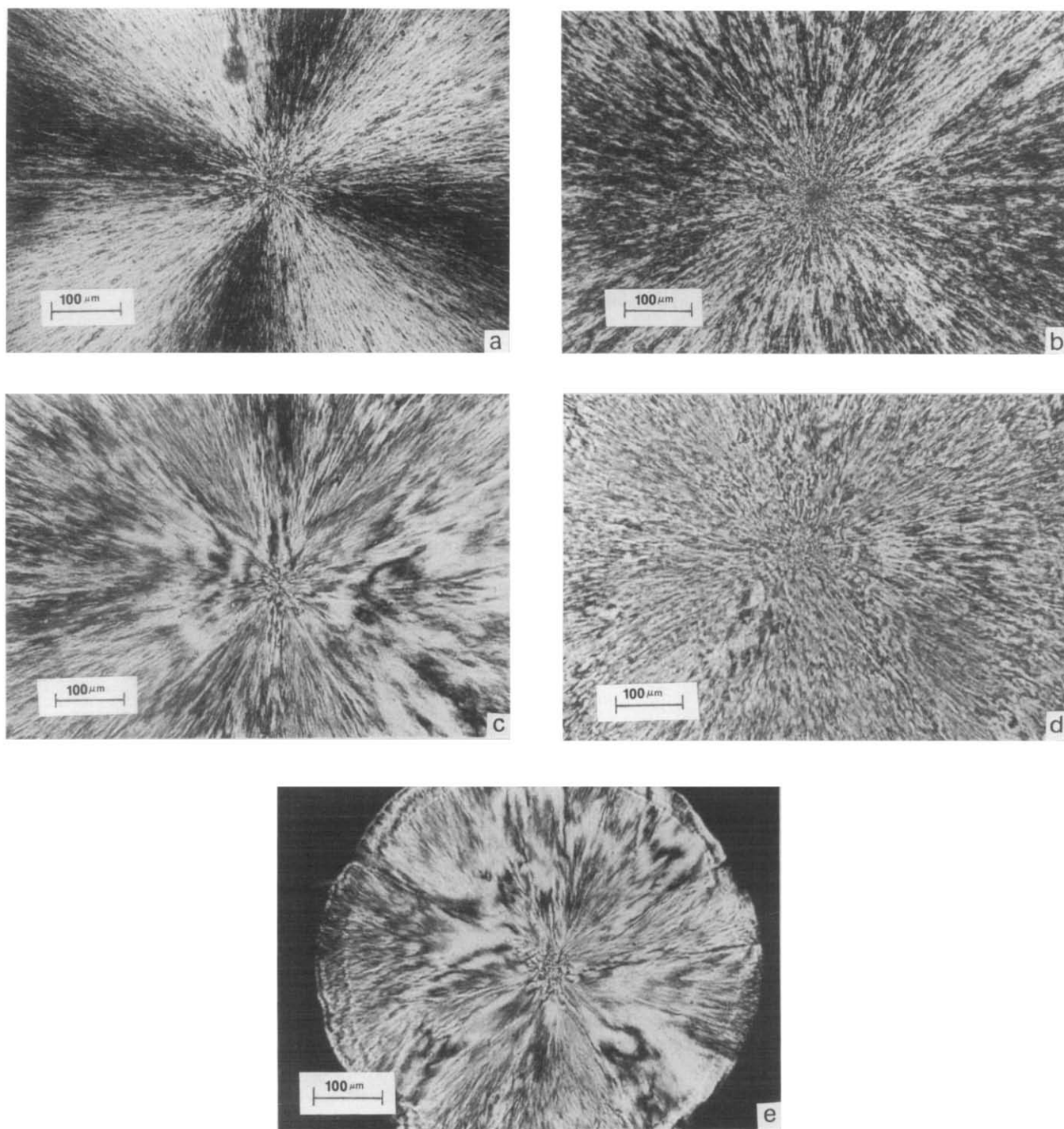


Figure 4 The crystalline morphology of the poly(ethylene oxide) fraction ($MW = 105\,000$) at different supercoolings in the vicinities of the regime transitions: (a) $\Delta T = 18.5$ K; (b) $\Delta T = 16.5$ K; (c) $\Delta T = 11$ K; (d) $\Delta T = 9.5$ K; and (e) $\Delta T = 7.5$ K

has been discussed, and it has been found that our approach (equations (1) and (7)) is also valid.

The morphological changes at the regime transitions have been studied. At $\Delta T = 17.5$ K, the change is between spherulites and intermediate states with the disappearance of the Maltese cross pattern; at $\Delta T = 10$ K, between intermediate states and hedrites; and, finally, at $\Delta T = 8.5$ K, between hedrites and single-crystal-like textures.

ACKNOWLEDGEMENTS

This work was partially supported by Exxon Educational Foundation. A very fruitful discussion with Professor

J. D. Hoffman on this topic led to considerable insight into the explanation for the reversion we observed. We would also like to thank Mr P. Giusti for his continuing assistance in microscopy.

REFERENCES

- 1 Kovacs, A. J. and Gonthier, A. *Kolloid Z. Z. Polym.* 1972, **250**, 530
- 2 Kovacs, A. J., Gonthier, A. and Straupe, C. *J. Polym. Sci., Polym. Symp.* 1975, **50**, 283
- 3 Kovacs, A. J., Straupe, C. and Gonthier, A. *J. Polym. Sci., Polym. Symp.* 1977, **59**, 31

- 4 Kovacs, A. J. and Straupe, C. *Faraday Discuss. Chem. Soc.* 1979, **68**, 225
- 5 Kovacs, A. J. and Straupe, C. *J. Cryst. Growth* 1980, **48**, 210
- 6 Cheng, S. Z. D. and Wunderlich, B. *J. Polym. Sci., Polym. Phys. Edn.* 1986, **24**, 577
- 7 Cheng, S. Z. D. and Wunderlich, B. *J. Polym. Sci., Polym. Phys. Edn.* 1986, **24**, 595
- 8 Cheng, S. Z. D., Bu, H.-S. and Wunderlich, B. *J. Polym. Sci., Polym. Phys. Edn.* 1988, **26**, 1947
- 9 Cheng, S. Z. D., Noid, D. W. and Wunderlich, B. *J. Polym. Sci., Polym. Phys. Edn.* 1989, **27**, 1149
- 10 Bu, H.-S., Cheng, S. Z. D. and Wunderlich, B. *Polym. Bull.* 1987, **16**, 567
- 11 Bu, H.-S., Cheng, S. Z. D. and Wunderlich, B. *Polymer* 1988, **29**, 1603
- 12 Cheng, S. Z. D., Bu, H.-S. and Wunderlich, B. *Polymer* 1988, **29**, 579
- 13 Cheng, S. Z. D. and Wunderlich, B. *Macromolecules* 1989, **22**, 1866
- 14 Maclaine, J. G. and Booth, C. *Polymer* 1975, **16**, 680
- 15 Maclaine, J. G. and Booth, C. *Polymer* 1975, **16**, 191
- 16 Mandelkern, L. and Stack, G. M. *Macromolecules* 1984, **17**, 871
- 17 Allen, R. C. and Mandelkern, L. *Polym. Bull.* 1987, **17**, 473
- 18 Hoffman, J. D. *Polymer* 1982, **23**, 656; 1983, **24**, 3
- 19 Pelzbauer, Z. and Galeski, A. *J. Polym. Sci. (C)* 1972, **38**, 23; see also Hoffman, J. D. *Polymer* 1983, **24**, 3
- 20 Hoffman, J. D. and Miller, R. L. *Macromolecules* 1988, **21**, 3038
- 21 Hoffman, J. D., Davis, G. T. and Lauritzen, J. I. Jr in 'Treatise on Solid-State Chemistry', (Ed. N. B. Hannay), Plenum Press, New York, 1976, Vol. 3, Ch. 7
- 22 Phillips, P. J. and Vatansever, N. *Macromolecules* 1987, **20**, 2138
- 23 Goldenfeld, N. *Polym. Commun.* 1984, **25**, 47
- 24 Hoffman, J. D. *Polymer* 1985, **26**, 803
- 25 Sadler, D. M. *Polymer* 1987, **28**, 1440
- 26 Hoffman, J. D. *Macromolecules* 1986, **19**, 1124
- 27 Magill, J. H. and Li, H.-M. *Polymer* 1978, **19**, 418
- 28 Lovering, E. G. *J. Polym. Sci. (C)* 1970, **30**, 329
- 29 Devoy, C. and Mandelkern, L. *J. Polym. Sci. (A-2)* 1969, **7**, 1883
- 30 Lopez, L. C. and Wilkes, G. L. *Polymer* 1988, **29**, 106
- 31 de Gennes, P.-G. *J. Chem. Phys.* 1971, **55**, 672; see also 'Scaling Concepts in Polymer Physics', Cornell University Press, Ithaca, NY, 1979